PAPER

Fitting Self-Similar Traffic by a Superposition of MMPPs Modeling the Distribution at Multiple Time Scales

António NOGUEIRA[†a)], **Paulo SALVADOR**[†b)], **Rui VALADAS**[†c)], ***Regular Members,*** ***and*** **António PACHECO**[††d)], ***Nonmember***

SUMMARY Measuring and modeling network traffic is of key importance for the traffic engineering of IP networks, due to the growing diversity of multimedia applications and the need to efficiently support QoS differentiation in the network. Several recent measurements have shown that Internet traffic may incorporate long-range dependence and self-similar characteristics, which can have significant impact on network performance. Self-similar traffic shows variability over many time scales, and this behavior must be taken into account for accurate prediction of network performance. In this paper, we propose a new parameter fitting procedure for a superposition of Markov Modulated Poisson Processes (MMPPs), which is able to capture self-similarity over a range of time scales. The fitting procedure matches the complete distribution of the arrival process at each time scale of interest. We evaluate the procedure by comparing the Hurst parameter, the probability mass function at each time scale, and the queuing behavior (as assessed by the loss probability and average waiting time), corresponding to measured traffic traces and to traces synthesized according to the proposed model. We consider three measured traffic traces, all exhibiting self-similar behavior: the well-known pOct Bellcore trace, a trace of aggregated IP WAN traffic, and a trace corresponding to the popular file sharing application Kazaa. Our results show that the proposed fitting procedure is able to match closely the distribution over the time scales present in data, leading to an accurate prediction of the queuing behavior.

key words: *Traffic modeling, self-similar, time scale, Markov Modulated Poisson Process.*

1. Introduction

The growing diversity of services and applications in the Internet places a strong requirement on the use of efficient design and control procedures. In particular, the main characteristics of the supported traffic must be known with sufficient detail. Several recent studies have shown that Internet traffic may exhibit properties of self-similarity and long-range dependence (LRD) [1]–[7]. In general, self-similarity implies long-range dependence and vice-versa. Self-similar traffic shows identical statistical characteristics over a wide range of time scales, which may have a significant impact on network performance. Therefore, it is important to make frequent measurements of packet flows and to describe them through appropriate traffic models.

Manuscript received May 27, 2003.
Manuscript revised October 14, 2003.
Final manuscript received November 15, 2003.

[†]University of Aveiro / Institute of Telecommunications Aveiro, Campus de Santiago, 3810-193 Aveiro, Portugal.
[††]Instituto Superior Técnico - UTL, Department of Mathematics and CEMAT, Av. Rovisco Pais, 1049-001 Lisboa, Portugal.
a) E-mail: nogueira@av.it.pt
b) E-mail: salvador@av.it.pt
c) E-mail: rv@det.ua.pt
d) E-mail: apacheco@math.ist.utl.pt

The impact of LRD on network performance has been addressed by several works . References [5], [8]–[10] study the case of a single queue and conclude that the buffer occupancy is not affected by autocovariance lags that are beyond the so-called critical time scale (CTS) or correlation horizon (CH), which depends on system parameters such as the buffer capacity. Similar conclusions are observed for the case of tandem queues in [11]. Thus, matching the LRD is only required within the time scales specific to the system under study. One of the consequences of this result is that more traditional traffic models, such as Markov Modulated Poisson Processes (MMPPs), can still be used to model traffic exhibiting LRD. The use of MMPPs also benefits from the existence of several tools for calculating the queuing behavior and the effective bandwidth.

In this paper we propose a new parameter fitting procedure for a superposition of Markov Modulated Poisson Processes (MMPPs), which captures self-similar behavior over a range of time scales. Each MMPP models a specific time scale. The parameter fitting procedure matches, at each time scale, an MMPP to a probability mass function (PMF) that describes the contribution of that time scale to the overall traffic behavior. The number of states of each MMPP is not fixed a priori; it is determined as part of the fitting procedure. The accuracy of the fitting procedure is evaluated by applying it to several measured traffic traces that exhibit self-similar behavior: the well-known pOct Bellcore trace, a trace of aggregated IP WAN traffic, and a trace corresponding to the file sharing application Kazaa. We selected the Kazaa application given its present popularity in the Internet. We compare the PMF at each time scale, and the queuing behavior (as assessed by the loss probability and average waiting time), corresponding to the measured and to synthetic traces generated from the inferred models. Our results show that the proposed fitting method is very effective in matching the PMF at the various time scales and leads to an accurate prediction of the queuing behavior.

When measuring network traffic data, we can either record the individual arrival instants or the number of arrivals in a predefined sampling (time) interval. The former approach brings more detail but the latter one has the advantage of producing a fixed amount of data that is known in advance. This allows the recording of longer traces, which clearly pays off the loss of detail in data recording, if the sampling interval is chosen appropriately. In this work, we consider discrete-time MMMPs (dMMPPs) instead of

continuous-time MMPPs, since they are more natural model for data corresponding to the number of arrivals in a sampling interval. Note that discrete-time and continuous-time MMPPs are basically interchangeable (through a simple parameter rescaling) as models for arrival processes, whenever the sampling interval used for the discrete-time version is small compared with the average sojourn times in the states of the modulating Markov chain.

Several fitting procedures have been proposed in the literature for estimating the parameters of MMPPs from empirical data ([12]–[21], among many others). However, most procedures only apply to 2-MMPPs (e.g. [12], [14], [15], [18]). This model can capture traffic burstiness but the number of states is not enough to reproduce variability over a wide range of time scales. On the other hand, the fitting procedures for MMPPs with an arbitrary number of states mainly concentrate on matching first- and/or second-order statistics, without addressing directly the issue of modeling on multiple time scales [13], [16], [17], [20], [21]. Yoshihara *et al.* [19] developed a fitting procedure for self-similar traffic based on the superposition of 2-MMPPs, that matches the variance over specified time scales. In this way, the resulting MMPP reproduces the variance-scale curve characteristic of self-similar processes. Kasahara [22] addressed in detail the queuing behavior achieved by this fitting procedure. Salvador *et al.* [21] proposed a fitting procedure that matches simultaneously the autocovariance and marginal distribution of the packet counts. The resulting MMPP is constructed as the superposition of L 2-MMPPs matching the autocovariance, and one M-MMPP matching the marginal distribution. The autocovariance modeling is such that each 2-MMPP (in the set of L 2-MMPPs) models a characteristic time constant (also called time scale) of the autocovariance function. In this paper we develop a procedure that matches the complete distribution of the packet counts at each time scale. Here, however, the concept of time scale is not directly related to second-order statistics; instead it refers to the characterization of the traffic process when aggregated over a number of time intervals. Thus, the proposed fitting method addresses the scaling paradigm in a more natural way than the one proposed in [21], achieving even higher accuracy in the fitting of self-similar traffic, although usually including a higher number of parameters in the resulting MMPP.

The paper is organized as follows. Section 2 introduces self-similarity and long-range dependence, motivating the need for a traffic model that matches the different time scales of the data. Section 3 gives the required background on MMPPs. Section 4 presents the various steps of the parameter fitting procedure. Section 5 briefly describes the data traces used in the numerical evaluation and in section 6 we discuss the results. Finally, section 7 presents the main conclusions.

2. Self-similarity, long-range dependence, and time scales

Consider the continuous-time process $Y(t)$ representing the traffic volume (e.g. in bytes) from time 0 up to time t and let $X(t) = Y(t) - Y(t-1)$ be the corresponding increment process (e.g. in bytes/second). Consider also the sequence $X^{(m)}(k)$ which is obtained by averaging $X(t)$ over non-overlapping blocks of length m, that is

$$X^{(m)}(k) = \frac{1}{m}\sum_{i=1}^{m} X((k-1)m+i), k = 1, 2, ... \quad (1)$$

The fitting procedure developed in this work will be based on the aggregated processes $X^{(m)}(k)$.

We start by introducing the notion of distributional self-similarity. $Y(t)$ is exactly self-similar when it is equivalent, in the sense of finite-dimensional distributions, to $a^{-H}Y(at)$, for all $t > 0$ and $a > 0$, where H $(0 < H < 1)$ is the Hurst parameter. Clearly, the process $Y(t)$ can not be stationary. However, if $Y(t)$ has stationary increments then again $X(k) = X^{(1)}(k)$ is equivalent, in the sense of finite-dimensional distributions, to $m^{1-H}X^{(m)}(k)$. This illustrates that a traffic model developed for fitting self-similar behavior must preferably enable the matching of the distribution on several time scales.

Long-range dependence is associated with stationary processes. Consider now that $X(k)$ is second-order stationary with variance σ^2 and autocorrelation function $r(k)$. Note that, in this case, $X^{(m)}(k)$ is also second-order stationary. The process $X(k)$ has long-range dependence (LRD) if its autocorrelation function is nonsummable, that is, $\sum_n r(n) = \infty$. Intuitively, this means that the process exhibits similar fluctuations over a wide range of time scales. Taking the case of the pOct Bellcore trace, it can be seen in Figure 1 that the fluctuations over the 0.01, 0.1 and 1s time scales are indeed similar.

Equivalently, one can say that a stationary process is LRD if its spectrum diverges at the origin, that is $f(v) \sim c_f|v|^{-\alpha}, v \to 0$. Here, α is a dimensionless scaling exponent, that takes values in $(0, 1)$; c_f takes positive real values and has dimensions of variance. On the other hand, a short range dependent (SRD) process is simply a stationary process which is not LRD. Such a process has $\alpha = 0$ at large scales, corresponding to white noise at scales beyond the so-called characteristic scale or correlation horizon. The Hurst parameter H is related with α by $H = (\alpha + 1)/2$.

There are several estimators of LRD. In this study we use the semi-parametric estimator developed in [23], which is based on wavelets. Here, one looks for alignment in the so-called Logscale Diagram (LD), which is a log-log plot of the variance estimates of the discrete wavelet transform coefficients representing the traffic process, against scale, completed with confidence intervals about these estimates at each scale. It can be thought of as a spectral estimator where large scale corresponds to low frequency. The main properties explored in this estimator are the stationarity and short-term correlations exhibited by the process of discrete wavelet transform coefficients and the power-law dependence in scale of the variance of this process. We will represent the scale by j and the logarithm of the variance

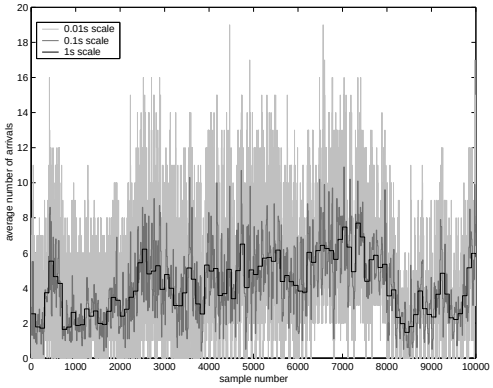

Fig. 1 LRD processes exhibit fluctuations over a wide range of time scales (Example: trace pOct).

estimate by y_j. Traffic is said to be LRD if, within the limits of the confidence intervals, the log of the variance estimates fall on a straight line, in a range of scales from some initial value j_1 up to the largest one present in data and the slope of the straight line, which is an estimate of the scaling exponent α, lies in $(0, 1)$.

There is a close relationship between long-range dependent and self-similar processes. In fact, if $Y(t)$ is self-similar with stationary increments and finite variance then $X(k)$ is long-range dependent, as long as $\frac{1}{2} < H < 1$. The process $X(k)$ is said to be exactly second-order self-similar $(\frac{1}{2} < H < 1)$ if

$$r\left(n\right) = 1/2\left[\left(n+1\right)^{2H} - 2n^{2H} + \left(n-1\right)^{2H}\right] \quad (2)$$

for all $n \geq 1$, or is asymptotically self-similar if

$$r\left(n\right) \sim n^{-(2-2H)} L(n) \quad (3)$$

as $n \to \infty$, where $L(n)$ is a slowly varying function at infinity. In both cases the autocovariance decays hyperbolically, which indicates LRD. Any asymptotically second-order self-similar process is LRD, and vice-versa.

3. Markov Modulated Poisson Processes

The discrete-time Markov Modulated Poisson Process (dMMPP) is the discrete-time version of the popular (continuous-time) MMPP and may be regarded as an Markov random walk where the increments in each instant have a Poisson distribution whose parameter is a function of the state of the modulator Markov chain. More precisely, the (homogeneous) Markov chain $(Y, J) = \{(Y_k, J_k),\, k = 0, 1, \ldots\}$ with state space $\mathbb{N}_0 \times S$ is a dMMPP if and only if for $k = 0, 1, \ldots,$

$$\begin{aligned} P(Y_{k+1} = m,\, J_{k+1} = j | Y_k = n,\, J_k = i) = \\ = \begin{cases} 0 & m < n \\ p_{ij}\, e^{-\lambda_j} \frac{\lambda_j^{m-n}}{(m-n)!} & m \geq n \end{cases} \end{aligned} \quad (4)$$

for all $m, n \in \mathbb{N}_0$ and $i, j \in S$, with λ_j, $j \in S$, being nonnegative real constants and $\mathbf{P} = (p_{ij})$ being a stochastic matrix. Note that the distribution of $Y_{k+1} - Y_k$ given $J_{k+1} = j$ is Poisson with mean λ_j, so that λ_j represents the mean increment of the process Y when the modulating Markov chain is in state j.

Whenever (4) holds, we say that (Y, J) is a dMMPP with set of modulating states S and parameter (matrices) $\mathbf{P}$ and $\mathbf{\Lambda}$, and write

$$(Y, J) \sim \text{dMMPP}_S(\mathbf{P}, \mathbf{\Lambda}) \quad (5)$$

where $\mathbf{\Lambda} = (\lambda_{ij}) = (\lambda_i \delta_{ij})$, with δ being the Kronecker function, i.e., δ_{ij} is one if $i = j$ and is zero otherwise. The matrix $\mathbf{P}$ is the transition probability matrix of the modulating Markov chain J, whereas $\mathbf{\Lambda}$ is the matrix of Poisson arrival rates. If S has cardinality r, we say that (Y, J) is a dMMPP of order r (r-dMMPP). When, in particular, $S = \{1, 2, \ldots, r\}$ for some $r \in \mathbb{N}$, then

$$\mathbf{P} = \begin{bmatrix} p_{11} & p_{12} & \ldots & p_{1r} \\ p_{21} & p_{22} & \ldots & p_{2r} \\ \ldots & \ldots & \ldots & \ldots \\ p_{r1} & p_{r2} & \ldots & p_{rr} \end{bmatrix} \quad (6)$$

and

$$\mathbf{\Lambda} = \begin{bmatrix} \lambda_1 & 0 & \ldots & 0 \\ 0 & \lambda_2 & \ldots & 0 \\ \ldots & \ldots & \ldots & \ldots \\ 0 & 0 & \ldots & \lambda_r \end{bmatrix} \quad (7)$$

and we write simply that $(Y, J) \sim \text{r-dMMPP}_r(\mathbf{P}, \mathbf{\Lambda})$.

Consider now the superposition of L independent dMMPPs

$$(Y^{(l)}, J^{(l)}) \sim r_l\text{-dMMPP}_{r_l}(\mathbf{P}^{(l)}, \mathbf{\Lambda}^{(l)}) \quad (8)$$

where $l = 1, 2, \ldots, L$ and $J^{(1)}, J^{(2)}, \ldots, J^{(L)}$ are ergodic chains in steady-state and the dimension of each dMMPP is not necessarily the same. For $l = 1, 2, \ldots, L$ we denote by $\pi^{(l)} = \left[\pi_1^{(l)}\ \pi_2^{(l)} \ldots\ \pi_{r_l}^{(l)}\right]$ the stationary distribution of $J^{(l)}$.

The result of the superposition is the process

$$\begin{aligned} (Y, J) = \left(\sum_{l=1}^{L} Y^{(l)}, (J^{(1)}, J^{(2)}, \ldots, J^{(L)})\right) \\ \sim \text{dMMPP}_S(\mathbf{P}, \mathbf{\Lambda}) \end{aligned} \quad (9)$$

where

$$S = \{1, 2, \ldots, r_1\} \times \ldots \times \{1, 2, \ldots, r_L\} \quad (10)$$

$$\mathbf{P} = \mathbf{P}^{(1)} \otimes \mathbf{P}^{(2)} \otimes \ldots \otimes \mathbf{P}^{(L)} \quad (11)$$

$$\mathbf{\Lambda} = \mathbf{\Lambda}^{(1)} \oplus \mathbf{\Lambda}^{(2)} \oplus \ldots \oplus \mathbf{\Lambda}^{(L)} \quad (12)$$

where $r_1, r_2, \ldots, r_L$, represent the dimensions of each one of the L dMMPPs, with $\oplus$ and $\otimes$ denoting the Kronecker sum and the Kronecker product, respectively. Note that the Markov chain J is also in steady-state.

In our approach L, that represents the number of time

scales considered, is fixed *a priori* and the dimensions of the dMMPPs, $r_1, r_2, \ldots, r_L$, are computed as part of the fitting procedure.

The dMMPP is a particular case of the discrete-time batch Markovian arrival process (usually denoted by D-BMAP) proposed by Blondia and Casals [24]. These processes and queues fed by them have received a great deal of attention (see, e.g., [25]–[33] and references therein). In particular, we note their use in explaining long range dependence [28].

4. Inference Procedure

The inference procedure estimates one dMMPP for each time scale that matches a probability mass function (PMF) characteristic of that time scale. The resulting dMMPP is obtained from the superposition of all dMMPPs inferred for each time scale. This inference procedure is closely related to the notion of distributional self-similarity. The flowchart of the inference method is represented in figure 2 where, basically, four steps can be identified: (i) compute the data sequences (corresponding to the average number of arrivals per time interval) at each time scale; (ii) calculate the empirical PMF at the largest time scale and infer its dMMPP; (iii) for all other time scales (going from the largest to the smallest one), calculate the empirical PMF, deconvolve it from the empirical PMF of the previous time scale and infer a dMMPP that matches the resulting PMF; and (iv) calculate the final dMMPP through superposition of the dMMPPs inferred for each time scale. We will describe these steps in detail in the next subsections. The time interval at the smallest time scale, Δt, the number of time scales, L, and the level of aggregation, a, are given apriori.

4.1 Calculation of the data aggregates

The procedure starts by computing the data sequence corresponding to the average number of arrivals in the smallest time scale, $D^{(1)}(k), k = 1, 2, \ldots, N$. Then, it calculates the data sequences of the remaining time scales, $D^{(l)}(k), l = 2, ..., L$, corresponding to the average number of arrivals in intervals of length $\Delta t a^{(l-1)}$. This is given by

$$D^{(l)}(k) = \begin{cases} \Psi\left(\frac{1}{a}\sum_{i=0}^{a-1} D^{(l-1)}(k+i)\right), & \frac{k-1}{a} \in I\!N_0 \\ D^{(l)}(k-1), & \frac{k-1}{a} \notin I\!N_0 \end{cases} \quad (13)$$

where $\Psi(x)$ represents round toward the integer nearest x. Note that the block length of equation (1) is related with a and l by $m = a^{l-1}$. Note also that all data sequences have the same length N and that $D^{(l)}(k)$ is formed by sub-sequences of a^{l-1} successive equal values; these sub-sequences will be called *l-sequences*. The empirical distribution of $D^{(l)}(k)$ will be denoted by $\hat{p}^{(l)}(x)$.

4.2 Calculation of the PMFs

This step infers the PMFs that, at each time scale, must be fitted to a dMMPP. For the largest time scale, this PMF is simply the empirical one. For all other time scales l, $l = 1, 2, ..., L-1$, the associated dMMPP will model only the traffic components due to that scale. For time scale l, these traffic components can be obtained through deconvolution of the empirical PMFs of this time scale and of previous time scale $l+1$, i.e.,

$$\hat{f}_p^{(l)}(x) = \left[\hat{p}^{(l)} \otimes^{-1} \hat{p}^{(l+1)}\right](x) \quad (14)$$

However, this may result in negative arrival rates for the dMMPP$^{(l)}$, which will occur whenever

$$\min\left\{x : \hat{p}^{(l+1)}(x) > 0\right\} < \min\left\{x : \hat{p}^{(l)}(x) > 0\right\} \quad (15)$$

To correct this, the dMMPP$^{(l)}$ will be fitted to

$$\hat{f}^{(l)}(x) = \hat{f}_p^{(l)}\left(x + e^{(l)}\right) \quad (16)$$

where $e^{(l)} = \min\left(0, \min\left\{x : \hat{f}_p^{(l)}(x) > 0\right\}\right)$, which assures $\hat{f}^{(l)}(x) = 0$, $x < 0$. These additional factors are removed in the final step of the inference procedure.

4.3 Parameter inference

The first step in the inference of the dMMPP$^{(l)}$ parameters, $l = 1, 2, ..., L$, is the approximation of $\hat{f}^{(l)}$ by a weighted sum of Poisson probability functions. This resorts to an algorithm, introduced in [21], that progressively subtracts a Poisson probability function from $\hat{f}^{(l)}$. The main steps of this algorithm are depicted in the flowchart of figure 3 and will be explained in the next paragraphs.

Let the i^{th} Poisson probability function, with mean $\varphi_i^{(l)}$, be represented by $g_{\varphi_i^{(l)}}(x)$ and define $h_{(i)}^{(l)}(x)$ as the difference between $\hat{f}^{(l)}(x)$ and the weighted sum of Poisson probability functions at the i^{th} iteration. Initially, we set $h_{(1)}^{(l)}(x) = \hat{f}^{(l)}(x)$ and, in each step, we first detect the maximum of $h_{(i)}^{(l)}(x)$. The corresponding x-value, $\varphi_i = [h_{(i)}^{(l)}]^{-1}\left(\max h_{(i)}^{(l)}(x)\right)$, will be considered the i^{th} Poisson rate of the d$MMPP^{(l)}$. We then calculate the weights of each Poisson probability function, $\vec{w}_i^{(l)} = \left[w_{1i}^{(l)}, w_{2i}^{(l)}, ..., w_{ii}^{(l)}\right]$, through the following set of linear equations:

$$\hat{f}^{(l)}(\varphi_m^{(l)}) = \sum_{j=1}^{i} w_{ji}^{(l)} g_{\varphi_j^{(l)}}(\varphi_m^{(l)}) \quad (17)$$

for $m = 1, ..., i$ and $l = 1, ..., L$. This assures that the fitting between $\hat{f}^{(l)}(x)$ and the weighted sum of Poisson probability functions is exact at $\varphi_m^{(l)}$ points, for $m = 1, 2, \ldots, i$. The final step in each iteration is the calculation of the new difference function

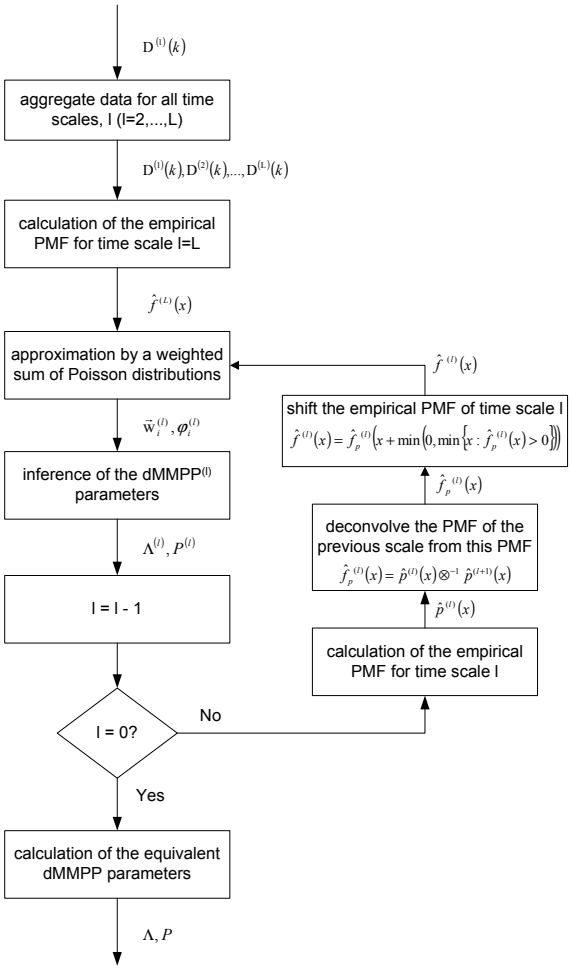

Fig. 2 Flow diagram of the inference procedure.

$$h_{(i+1)}^{(l)}(x) = \hat{f}^{(l)}(x) - \sum_{j=1}^{i} w_{ji}^{(l)} g_{\varphi_j^{(l)}}(x). \qquad (18)$$

The algorithm stops when the maximum of $h_{(i)}^{(l)}(x)$ is lower than a pre-defined percentage of the maximum of $\hat{f}^{(l)}(x)$ and r_l, the number of states of the dMMPP, is made equal to i.

Note that the number of states of each dMMPP depends on the level of accuracy employed in the approximation of the empirical PMF by the weighted sum of Poisson probability functions.

After r_l has been determined, the parameters $\pi_j^{(l)}$ and $\lambda_j^{(l)}$, $j = 1, 2, \ldots, r_l$, of the r_l − dMMPP, are set equal to

$$\pi_j^{(l)} = w_{jr_l}^{(l)} \qquad \text{and} \qquad \lambda_j^{(l)} = \varphi_j^{(l)}. \qquad (19)$$

The next step is to associate, for each time scale l, one of the dMMPP$^{(l)}$ states with each time slot of the arriving process. Recall the data sequences aggregated at time scale l have a^{l-1} successive equal values called l-sequences. The state assignment process considers only the first time interval of each l-sequence, defined by $i = a^{l-1}(k-1)+1, k \in$

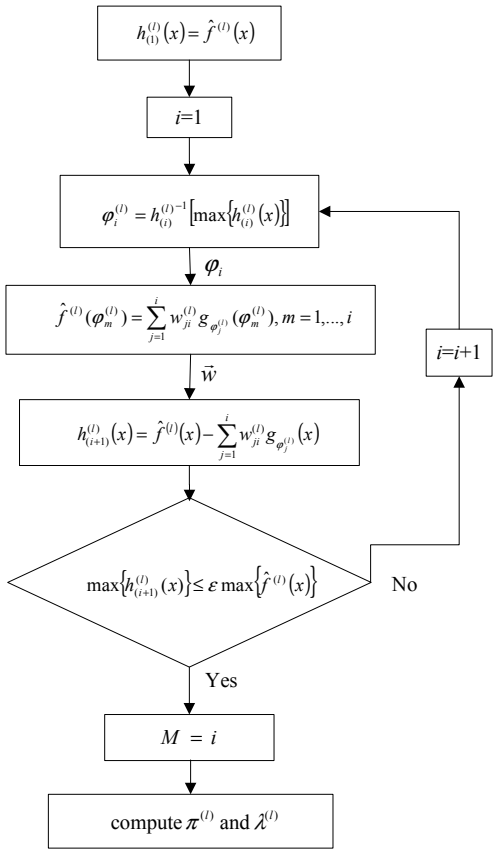

Fig. 3 Algorithm for calculating the number of states and the Poisson arrival rates of the dMMPP$^{(l)}$.

$I\!N, i \leq N$. The state that is assigned to l-sequence i is calculated randomly according to the probability vector $\vec{\theta}^{(l)}(i) = \left\{\theta_1^{(l)}(i), \ldots, \theta_{r_l}^{(l)}(i)\right\}$, with

$$\theta_i^{(l)}(n) = \frac{g_{\lambda_i^{(l)}}\left(D^l(i)\right)}{\sum_{j=1}^{r_l} g_{\lambda_j^{(l)}}(D^l(i))}, \qquad (20)$$

where $n = 1, ..., r_l$, and $g_\lambda(y)$ represents a Poisson probability distribution function with mean λ. The elements of this vector represent the probability that the state j had originated the number of arrivals $D^{(l)}(k)$ at time slot k from time scale l.

After this step, we infer the dMPPP$^{(l)}$ transition probabilities, $p_{ij}^{(l)}, i, j = 1, ..., r_l$, by counting the number of transitions between each pair of states. If $n_{ij}^{(l)}$ represents the number of transitions from state i to state j, corresponding to the dMPPP$^{(l)}$, then

$$p_{ij}^{(l)} = \frac{n_{ij}^{(l)}}{\sum_{m=1}^{r_l} n_{mj}^{(l)}}, j = 1, ..., r_l \qquad (21)$$

The transition probability and the Poisson arrival rate matrices of the dMPPP$^{(l)}$ are then given by

$$\mathbf{P}^{(l)} = \begin{bmatrix} p_{11}^{(l)} & p_{12}^{(l)} & \dots & p_{1r_l}^{(l)} \\ p_{21}^{(l)} & p_{22}^{(l)} & \dots & p_{2r_l}^{(l)} \\ \dots & \dots & \dots & \dots \\ p_{r_l1}^{(l)} & p_{r_l2}^{(l)} & \dots & p_{r_lr_l}^{(l)} \end{bmatrix} \quad (22)$$

and

$$\mathbf{\Lambda}^{(l)} = \begin{bmatrix} \lambda_1^{(l)} & 0 & \dots & 0 \\ 0 & \lambda_2^{(l)} & \dots & 0 \\ \dots & \dots & \dots & \dots \\ 0 & 0 & \dots & \lambda_{r_l}^{(l)} \end{bmatrix} \quad (23)$$

with $l = 1, ..., L$.

4.4 Construction of the final dMMPP model

The final dMMPP process is constructed using equations (11) and (12), where the matrices $\mathbf{\Lambda}^{(l)}$ and $\mathbf{P}^{(l)}$, $l = 1, ..., L$, were calculated in the last subsection. However, the additional factors introduced in sub-section 4.2 must be removed. Thus,

$$\mathbf{\Lambda} = \mathbf{\Lambda} - \sum_{l=1}^{L-1} e^{(l)} \cdot \mathbf{I} \quad (24)$$

where $\mathbf{I}$ is the identity matrix.

5. Measured traffic traces

The evaluation of fitting procedure will be based on three measured traffic traces. Two traces are of aggregated IP traffic: (i) the well-known and publicly available pOct LAN trace from Bellcore [1] and (ii) a trace corresponding to the downstream Internet access traffic of approximately 65 simultaneous users, measured at the access link of a Portuguese ISP (to an ADSL network). The third trace is from the Kazaa application (10 simultaneous users) and was also measured at the above access link. We have included this application given the fact that an increasing percentage of the overall Internet traffic belongs to peer-to-peer protocols of the same type as Kazaa. For all our measurements, the traffic analyzer was a 1.2 GHz AMD Athlon PC, with 1.5 Gbytes of RAM and running WinDump; we recorded the arrival instant and the IP header of each packet. No packet drops were reported by WinDump in all measurements. The main characteristics of the selected traces are described in Table 1.

All traces exhibit self-similar behavior. For example, taking the case of trace pOct, the analysis of its autocovariance function (Figure 4) lead us to suspect that it exhibits LRD, due to the slow decay for large time lags. This is confirmed by the scaling analysis, since the y_j values in the Logscale Diagram, are aligned between a medium octave (7) and octave 14, the highest one present in data (Figure 5). Recall that the y_j values are logarithms of the variance estimates of the discrete wavelet transform coefficients that represent the traffic process. A similar analysis was made for the other traces, also revealing the same self-similar (LRD) behavior.

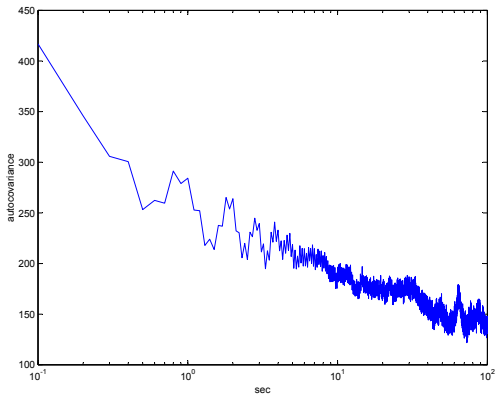

Fig. 4 Autocovariance of packet counts, trace pOct.

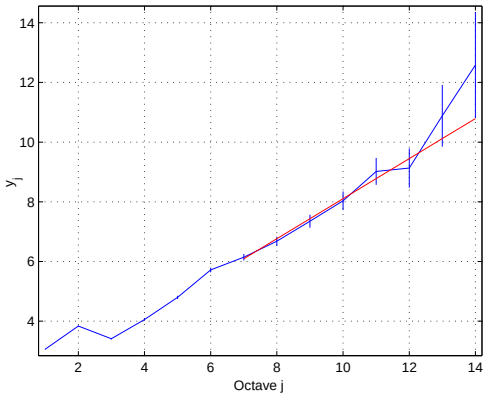

Fig. 5 Second order Logscale Diagram, trace pOct.

6. Numerical Results

The suitability of the proposed dMMPP fitting procedure is assessed using several criteria: (i) comparing the Hurst parameters of the original and synthesized (from the inferred dMMPP) data traces; (ii) comparing the probability functions of the average number of arrivals in different time scales, obtained for the original and synthesized traces and (iii) comparing the queuing behavior, in terms of packet loss ratio (PLR) and average waiting time in queue (AWT), of the original and synthesized traces, using trace-driven simulation. We have resorted to simulation since, in our case, the packet processing times are not necessarily multiples of the sampling interval, as would be required for using the available theoretical results of dMMPPs.

All simulations were carried out using a fixed packet length equal to the mean packet length of the trace. For all traces, the sampling interval of the counting process was chosen to be 0.1s and three different time scales were considered: 0.1s, 0.2s and 0.4s. For each trace, the estimation procedure took less than 1 minute, using a MATLAB implementation running in the PC described above, which shows that the procedure is computationally very efficient.

In order to verify that the proposed fitting approach captures the self-similar behavior, we compare in Table 2

Trace name	Capture period	Trace size (pkts)	Mean rate (byte/s)	Mean pkt size (bytes)
October	Bellcore trace	1 million	322790	568
ISP	10.26pm to 10.49pm, October 18^{th}2002	1 million	583470	797
Kaaza	10.26pm to 11.31pm, October 18^{th}2002	0.5 million	131140	1029

Table 1 Main characteristics of measured traces.

Trace	original	fitted
October	0.941 (6,12)	0.962 (6,12)
ISP	0.745 (6,13)	0.784 (4,13)
Kazaa	0.783 (6,12)	0.773 (2,12)

Table 2 Comparison between Hurst parameter values

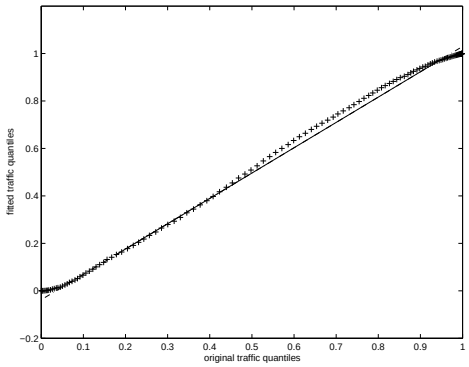

Fig. 6 Q-Q plot of the cumulative probability function at the smallest time scale, trace pOct.

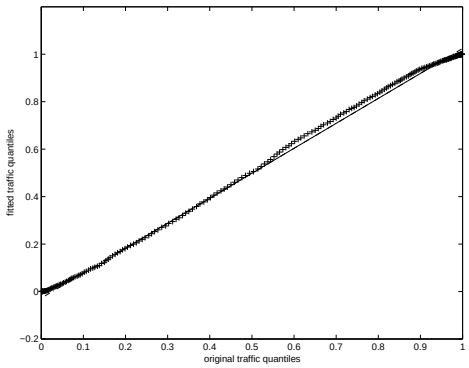

Fig. 7 Q-Q plot of the cumulative probability function at the intermediate time scale, trace pOct.

the Hurst parameters estimated for the original and fitted traffic, for each one of the three selected data traces. Table 2 also includes the range of time scales where the y_j follow a straight line, inside brackets near to the corresponding Hurst parameter value. There is a very good agreement between the Hurst parameter values of the original and fitted traffic, so LRD behavior is indeed well captured by our model.

The next evaluation criteria is based on the comparison between the PMFs of the original and fitted traces, for different time scales. Starting with trace pOct, it can be seen in Figures 6, 7, 8, 9, 10, 11 and 12 that there is a good

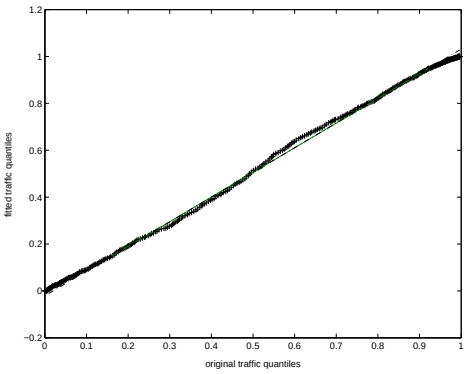

Fig. 8 Q-Q plot of the cumulative probability function at the largest time scale, trace pOct.

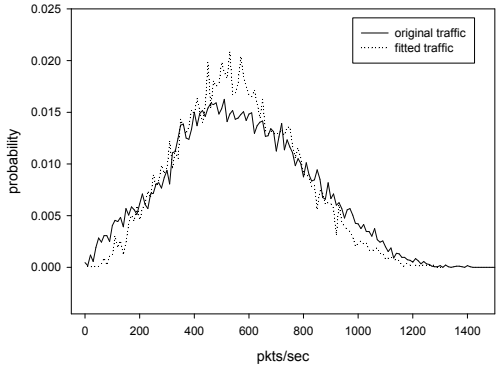

Fig. 9 Probability mass function at the smallest time scale, trace pOct.

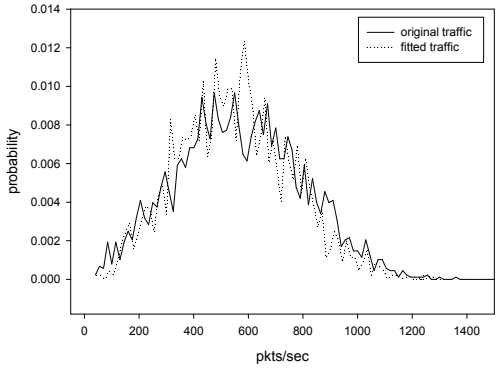

Fig. 10 Probability mass function at the intermediate time scale, trace pOct.

agreement between the probability functions of the original and fitted traces, for all time scales. We used three different types of graphical comparison to show the accuracy of

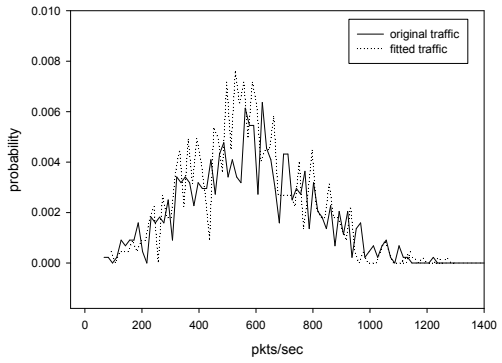

Fig. 11 Probability mass function at the largest time scale, trace pOct.

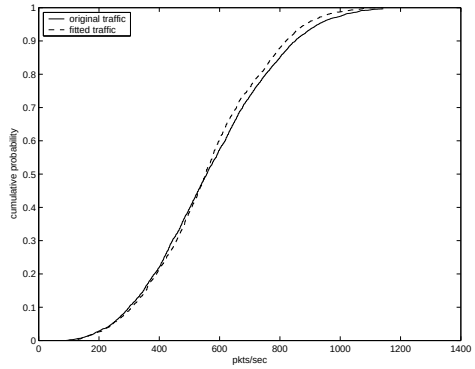

Fig. 12 Cumulative probability function at the largest time scale, trace pOct.

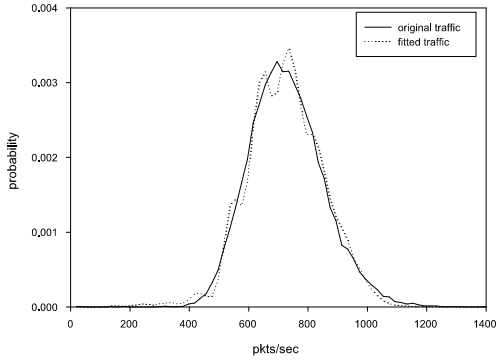

Fig. 13 Probability mass function at the smallest time scale, trace ISP.

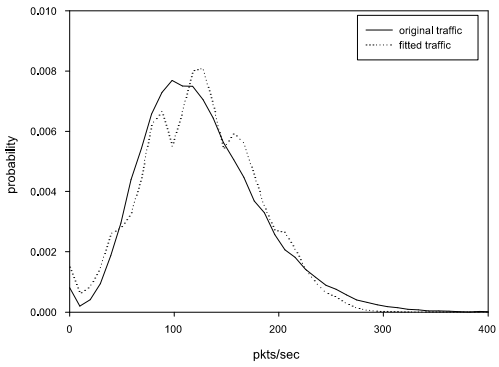

Fig. 14 Probability mass function at the smallest time scale, trace Kazaa.

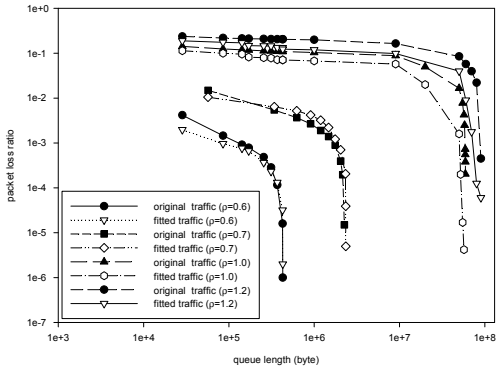

Fig. 15 Packet loss ratio, trace pOct.

the inference procedure in the fitting of the original trace PMF: PMF plot, QQ-plot and CDF plot. Recall that the fitting procedure explicitly aimed at matching the PMF at the various time scales, so the obtained results confirm that the procedure is effective in performing this task. Due to space limitations, for the case of the ISP and Kazaa traces we only show the comparison between the probability functions at the smallest time scale, in Figures 13 and 14. However, a good agreement also exists at the three times scales.

Considering now the queuing behavior, we compare the PLR and the AWT obtained, through trace-driven simulation, with the original and fitted traces. Two different sets of utilization ratios were used in the simulations: for traces pOct and Kazaa, we used $\rho = 0.6$ and $\rho = 0.7$ and for trace ISP the selected values were $\rho = 0.8$ and $\rho = 0.9$. This is due to the lower burstiness of the ISP traffic, which leads to lower packet losses for the same link utilization. Besides these utilization ratio values, we have also run simulations with $\rho = 1.0$ and $\rho = 1.2$, for all traces, in order to assess how the generated dMMPPs capture the performance at high utilization ratio values.

From figures 15 and 16 it can be seen that, for trace pOct, the PLR is very well approximated by the fitted dMMPP for the lower utilization ratios ($\rho = 0.6$ and $\rho = 0.7$) but the accuracy degrades at higher utilization ratios. The same behavior occurs for the AWT, but generally the agreement of the AWT curves is less accurate than that of the PLR curves, even for low utilization ratios. For trace ISP the results are illustrated in figures 17 and 18. The agreement between the curves corresponding to the original and fitted traces is good for both performance metrics and for all utilization ratio values, specially for $\rho = 0.6$ and $\rho = 0.7$. For trace Kazaa the results are depicted in figures 19 and 20. In this case, the agreement between the curves is only good for the $\rho = 0.6$ and $\rho = 0.7$ utilization ratios, beginning to degrade as the utilization ratio increases. This behavior is similar to the one observed for trace pOct. Thus, in general, the results are good except for the highest utilization ratios where some deviations can occur. At these values,

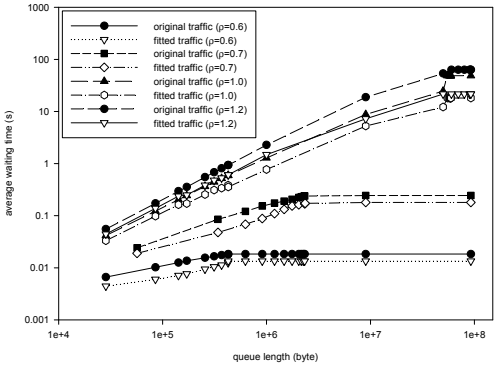

Fig. 16 Average waiting time in queue, trace pOct.

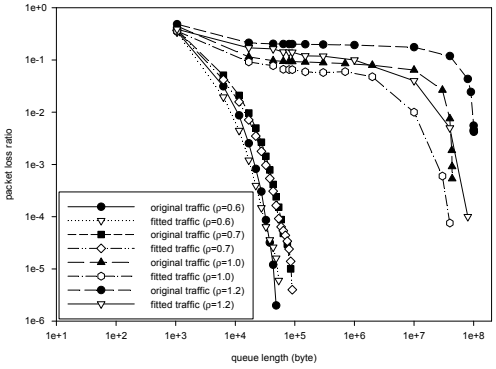

Fig. 19 Packet loss ratio, trace Kazaa.

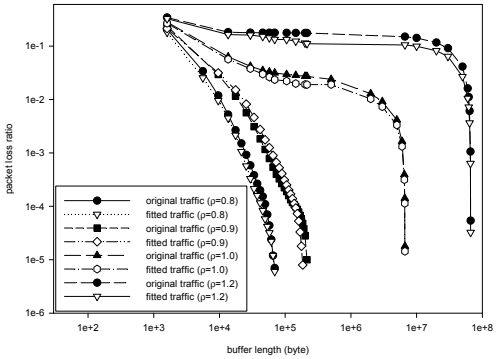

Fig. 17 Packet loss ratio, trace ISP.

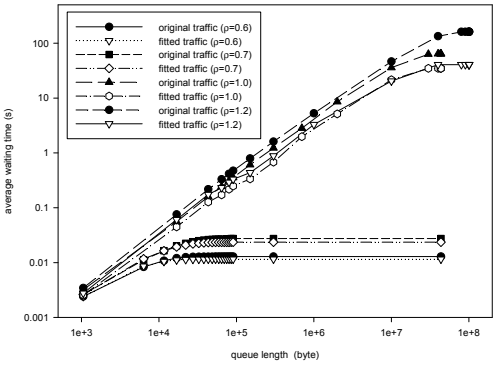

Fig. 20 Average waiting time in queue, trace Kazaa.

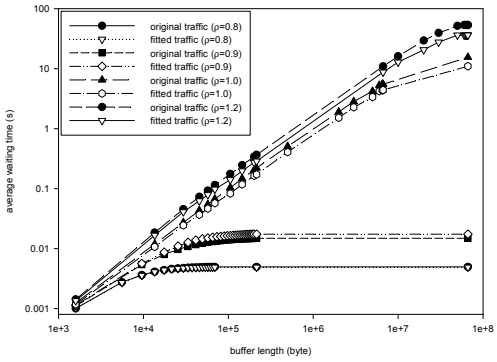

Fig. 18 Average waiting time in queue, trace ISP.

the buffer occupancies are very high and the sensitivity of the results becomes larger; however, the packet losses and waiting times are very high, even unrealistic for operational networks.

As a final remark, we can say that the proposed fitting approach provides a close match of the Hurst parameters and probability mass functions at each time scale, and this agreement reveals itself sufficient to drive a good queuing performance in terms of packet loss ratio and average waiting time in queue. The computational complexity of the fitting method is also very small.

7. Conclusions

We have proposed a new parameter fitting procedure for a superposition of Markov Modulated Poisson Processes (MMPPs), which is able to capture self-similarity over a range of time scales. The fitting procedure matches the complete distribution of the arrival process at each time scale of interest. We evaluated the procedure by comparing the Hurst parameter, the probability mass function at each time scale, and the queuing behavior (as assessed by the loss probability and average waiting time), corresponding to measured traffic traces and to traces synthesized according to the proposed model. Three measured traffic traces were considered, all exhibiting self-similar behavior: the well-known pOct Bellcore trace, a trace of aggregated IP WAN traffic, and a trace corresponding to the popular file sharing application Kazaa. Our results show that the proposed fitting procedure is able to match closely the distribution over the time scales present in data, leading to an accurate prediction of the queuing behavior.

Acknowledgement

The authors would like to thank the anonymous referees for their valuables comments and suggestions. This research was supported in part by Fundação para a Ciência e a Tecnologia, the project POSI/42069/CPS/2001, and the grant

BD/19781/99.

References

[1] W. Leland, M. Taqqu, W. Willinger, and D. Wilson, "On the self-similar nature of Ethernet traffic (extended version)," *IEEE/ACM Transactions on Networking*, vol. 2, no. 1, pp. 1–15, Feb. 1994.

[2] J. Beran, R. Sherman, M. Taqqu, and W. Willinger, "Long-range dependence in variable-bit rate video traffic," *IEEE Transactions on Communications*, vol. 43, no. 2/3/4, pp. 1566–1579, 1995.

[3] M. Crovella and A. Bestavros, "Self-similarity in World Wide Web traffic: Evidence and possible causes," *IEEE/ACM Transactions on Networking*, vol. 5, no. 6, pp. 835–846, Dec. 1997.

[4] V. Paxson and S. Floyd, "Wide-area traffic: The failure of Poisson modeling," *IEEE/ACM Transactions on Networking*, vol. 3, no. 3, pp. 226–244, June 1995.

[5] B. Ryu and A. Elwalid, "The importance of long-range dependence of VBR video traffic in ATM traffic engineering: Myths and realities," *ACM Computer Communication Review*, vol. 26, pp. 3–14, Oct. 1996.

[6] W. Willinger, M. Taqqu, R. Sherman, and D. Wilson, "Self-similarity through high-variability: Statistical analysis of Ethernet LAN traffic at the source level," *IEEE/ACM Transactions on Networking*, vol. 5, no. 1, pp. 71–86, Feb. 1997.

[7] W. Willinger, V. Paxson, and M. Taqqu, *Self-similarity and Heavy Tails: Structural Modeling of Network Traffic*, A Practical Guide to Heavy Tails: Statistical Techniques and Applications. Birkhauser, 1998.

[8] D. P. Heyman and T. V. Lakshman, "What are the implications of long range dependence for VBR video traffic engineering?," *IEEE/ACM Transactions on Networking*, vol. 4, no. 3, pp. 301–317, June 1996.

[9] A. Neidhardt and J. Wang, "The concept of relevant time scales and its application to queuing analysis of self-similar traffic," in *Proceedings of SIGMETRICS'1998/PERFORMANCE'1998*, 1998, pp. 222–232.

[10] M. Grossglauser and J. C. Bolot, "On the relevance of long-range dependence in network traffic," *IEEE/ACM Transactions on Networking*, vol. 7, no. 5, pp. 629–640, Oct. 1999.

[11] A. Nogueira and R. Valadas, "Analyzing the relevant time scales in a network of queues," in *SPIE's International Symposium ITCOM 2001*, Aug. 2001.

[12] K. Meier-Hellstern, "A fitting algorithm for Markov-modulated Poisson process having two arrival rates," *European Journal of Operational Research*, vol. 29, 1987.

[13] P. Skelly, M. Schwartz, and S. Dixit, "A histogram-based model for video traffic behaviour in an ATM multiplexer," *IEEE/ACM Transactions on Networking*, pp. 446–458, Aug. 1993.

[14] R. Grünenfelder and S. Robert, "Which arrival law parameters are decisive for queueing system performance," in *International Teletraffic Congress, ITC 14*, 1994.

[15] S. Kang and D Sung, "Two-state MMPP modelling of ATM superposed traffic streams based on the characterisation of correlated interarrival times," *IEEE GLOBECOM'95*, pp. 1422–1426, Nov. 1995.

[16] A. Andersen and B. Nielsen, "A Markovian approach for modeling packet traffic with long-range dependence," *IEEE Journal on Selected Areas in Communications*, vol. 16, no. 5, pp. 719–732, June 1998.

[17] S. Li and C. Hwang, "On the convergence of traffic measurement and queuing analysis: A statistical-match and queuing (SMAQ) tool," *IEEE/ACM Transactions on Networking*, pp. 95–110, Feb. 1997.

[18] C. Nunes and A. Pacheco, "Parametric estimation in MMPP(2) using time discretization," *Proceedings of the 2nd Internation Symposium on Semi-Markov Models: Theory and Applications*, Dec. 1998.

[19] T. Yoshihara, S. Kasahara, and Y. Takahashi, "Practical time-scale fitting of self-similar traffic with Markov-modulated Poisson process," *Telecommunication Systems*, vol. 17, no. 1-2, pp. 185–211, 2001.

[20] P. Salvador and R. Valadas, "A fitting procedure for Markov modulated Poisson processes with an adaptive number of states," in *Proceedings of the 9th IFIP Working Conference on Performance Modelling and Evaluation of ATM & IP Networks*, June 2001.

[21] P. Salvador, A. Pacheco, and R. Valadas, "Multiscale fitting procedure using Markov modulated Poisson processes," *Telecommunications Systems*, vol. 23, no. 1-2, pp. 123–148, June 2003.

[22] S. Kasahara, "Internet traffic modeling: Markovian approach to self-similar traffic and prediction of loss probability for finite queues," *IEICE Transactions on Communications*, vol. E84-B, no. 8, pp. 2134–2141, 2001.

[23] D. Veitch and P. Abry, "A wavelet based joint estimator for the parameters of LRD," *IEEE Transactions on Information Theory*, vol. 45, no. 3, Apr. 1999.

[24] C. Blondia and O. Casals, "Statistical multiplexing of VBR sources: A matrix-analytic approach," *Performance Evaluation*, vol. 16, no. 1-3, pp. 5–20, 1992.

[25] C. Blondia, "A discrete-time batch Markovian arrival process as B-ISDN traffic model," *Belgian Journal of Operations Research, Statistics and Computer Science*, vol. 32, pp. 3–23, 1993.

[26] A.S. Alfa and S. Chakravarthy, "A discrete queue with the Markovian arrival process and phase type primary and secondary services," *Stochastic Models*, vol. 10, no. 2, pp. 437–451, 1994.

[27] N. Rananand, "Markov approximations to D-BMAPs: information-theoretic bounds on queueing performance," *Stochastic Models*, vol. 11, no. 4, pp. 713–734, 1995.

[28] F. Geerts and C. Blondia, "Superposition of Markov sources and long range dependence," in *Information Network and Data Communications: Proceedings of the IFIP/ICCC International Conference on Information Network and Data Communication*, F.A. Aagesen, H. Botnevik, and D. Khakhar, Eds. Chapman & Hall, 1996.

[29] I. Frigui, A.S. Alfa, and X. Xu, "Algorithms for computing waiting time distributions under different queue disciplines for the D-BMAP/PH/1," *Naval Research Logistics*, vol. 44, no. 6, pp. 559–576, 1997.

[30] A.S. Alfa, "Discrete time analysis of a MAP/PH/1 vacation queue with gated time-limited service," *Queueing Systems*, vol. 29, pp. 35–54, 1998.

[31] Ad Ridder, "Fast simulation of discrete time queues with Markov modulated batch arrivals and batch departures," *AEU International Journal of Electronics and Communications*, vol. 52, pp. 127–132, 1998.

[32] C. Herrmann, "The complete analysis of the discrete time finite DBMAP/G/1/N queue," *Performance Evaluation*, vol. 43, pp. 95–121, 2001.

[33] N.K. Kim, S.H. Chang, and K.C. Chae, "On the relationships among queue lengths at arrival, departure, and random epochs in the discrete-time queue with D-BMAP arrivals," *Operations Research Letters*, vol. 30, no. 6, pp. 25–32, 2002.

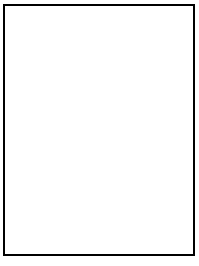

António Nogueira was born in Mozambique, on March 12, 1969. He graduated in Electronics and Telecommunications Engineering in 1992 and received the MSc. degree in Electronics and Telecommunications Engineering in 1997, both from University of Aveiro, Aveiro, Portugal. In 1995, he joined Institute of Telecommunications - pole of Aveiro as a researcher. He is currently an Assistant and a PhD. student at University of Aveiro. His main re-

search areas of interest are traffic modeling and network planning.

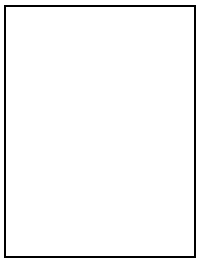

Paulo Salvador was born in Coimbra, Portugal, on February 17, 1975. He graduated in Electronics and Telecommunications Engineering in 1998 from University of Aveiro, Aveiro, Portugal. In 1998, he joined Institute of Telecommunications, Aveiro, Portugal, as a researcher. He is currently a PhD. student at University of Aveiro. His main research areas of interest are traffic modeling, network planning and Internet security.

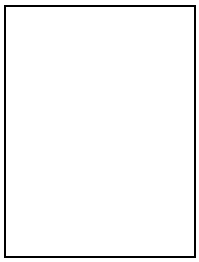

Rui Valadas graduated in Electrical and Computers Engineering, in 1986, from the Instituto Superior Técnico, Lisbon, Portugal, and received the Ph.D. degree from the University of Aveiro, Aveiro, Portugal, in 1996. He joined the University of Aveiro in 1986, where he is now an Associate Professor of the Department of Electronics and Telecommunications. He is also leader of the Networks and Multimedia Communications Group at the Institute of Telecommunications, Aveiro, Portugal. His main research interests are in the area of traffic engineering.

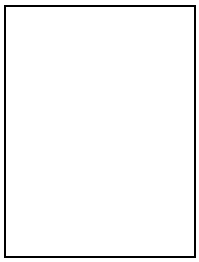

António Pacheco graduated in probability and statistics at Faculdade de Ciências, University of Lisbon, Portugal, in 1987, received the M.Sc. degree in applied mathematics from the IST (Instituto Superior Técnico, Technical University of Lisbon, Portugal) in 1991, and obtained the Ph.D. degree in operations research at Cornell University in 1994. He has been working at IST since 1987, where he is now Associate Professor at the Mathematics Department, and has been a full member of the Center for Mathematics and its Applications from IST since 1994. He has been teaching courses in stochastic processes, time series and engineering statistics at IST. His current research interests include stochastic processes, queueing theory, telecommunications networks, stochastic process control and stochastic automata. He is a member of INFORMS, SPE and AB-FLAD.